Optimizing magnetic hyperthermia respecting field safety conditions

Carlota Puig Acevedo, cpuigace7@alumnes.ub.edu
Facultat de Física, Universitat de Barcelona, Diagonal 645, 08028 Barcelona, Spain.

Advisor: Òscar Iglesias, oscariglesias@ub.edu

Abstract: A precise evaluation of magnetic nanoparticle heating under AC fields is essential to optimize hyperthermia treatments within physiologically safe limits. Standard models often rely on the uniaxial anisotropy approximation, assuming shape effects to dominate. However, we show that this assumption fails at low field amplitudes relevant to clinical conditions. Using computational simulations based on the Landau-Lifschitz-Gilbert equation implemented via OOMMF, we demonstrate that intrinsic magnetocrystalline anisotropy significantly influences the specific loss power (SLP), and that even minor deviations from the spherical shape can strongly affect heating efficiency. We will compare our results under the Thiesen-Jordan criterion to those obtained using the more commonly adopted Brezovich criterion, highlighting the importance of including intrinsic anisotropy, as well as controlling NP size and ensemble aspect ratio variability, when modeling hyperthermia performance under realistic safety constraints.
Keywords: Magnetic nanoparticles, Micromagnetism, Hysteresis, Cancer treatment, Biomedical applications, Simulation methods
SDGs: Good Health and well-being, quality education and industry, innovation and infrastructure

I. INTRODUCTION

Magnetic fluids have recently received attention for their use in clinical applications such as drug delivery, diagnosis, disease detection or cancer treatment via magnetic hyperthermia. The latter offers an attractive alternative for local therapy in cancer treatment as it has fewer side effects than traditional methods and can be used combined with radiation or chemotherapy treatments to improve their performance. Localized heating to $42-45°$C has been discovered to potentially kill tumor cells without harming healthy tissue.

The heat generation in magnetic hyperthermia arises from energy losses in NPs, which can be broadly categorized as Néel and Brownian relaxation losses. Since we consider the NPs to be fixed in this study, Brownian relaxation is irrelevant and excluded from the analysis. In Néel relaxation, heat is produced as the magnetic moments dissipate energy while aligning with an alternating magnetic field (AMF). The efficiency of this heating process is quantified by the specific absorption rate (SAR), also referred to as specific loss power (SLP), which represents the energy dissipated per unit time and per unit mass of NPs. The SLP is strongly dependent on both the amplitude and frequency of the applied field, as well as the intrinsic magnetic properties of the material.

For a magnetic field of amplitude H_{max} and frequency f, $SLP = A \cdot f/\rho$, where ρ is the density of the magnetic material and A stands for the hysteresis losses area, which can be computed as the area of the $M(H)$ loop. However, hyperthermia calculations are constrained by bio compatibility requirements. Several criteria have been proposed to establish a biological limit for the field-frequency product used in in-vivo applications. In the previous literature, it has been common to adopt the Brezovich criterion ($f \cdot H \leqslant 4.8 \times 10^8$ A/(m·s)) as a safety threshold to ensure patient safety. The following research departs from earlier works by choosing the Thiesen-Jordan criterion [1] ($f \cdot H \leqslant 1.8 \times 10^9$ A/(m·s)) to see how pushing the biological limit further may affect the heating capacity of NPs.

Magnetic anisotropy is a crucial parameter that determines the heat released by the NPs under the AC field because reasonable heat can only be obtained if a minimum field threshold is met. That is, $H_{max} \geqslant 0.5 H_K = \frac{2K_{eff}}{\mu_0 M_s}$ is required for significant heating [2]. Since calculating anisotropy conditions can be very complex, the common working procedure in hyperthermia simulation is to assume uniaxial anisotropy of NPs. Recent studies have shown that, while the uniaxial approach holds in high-range fields, it may fail in small-range fields. [3]

The aim of our work is to study heat generation using a less restrictive criterion and to evaluate its effects on the applicability of the uniaxial anisotropy approximation and in the proposal of a more realistic model involving both magnetocrystalline and shape anisotropy. The optimal NP sizes that maximize the SLP and the influence of NP shape deviations from sphericity will also be reported.

II. THEORETICAL FRAMEWORK AND SIMULATION DETAILS

A. Physical description of model

Under the application of alternating magnetic fields (AMFs) all magnetic materials can produce heat through hysteresis losses, related to the energy dissipated in each magnetization reversal cycle.

As particle size decreases into the single-domain regime at $T = 0$, the equilibrium magnetization direction is determined by the anisotropy contributions due to crys-

tal structure, particle shape, and surface effects. In the single-domain limit, the Stoner-Wohlfarth (SW) model [4] provides a simple description of magnetization reversal treating anisotropy as uniaxial. The model predicts coherent rotation of magnetization and ideal square hysteresis loops for non-interacting particles with easy axes aligned to the external field [5]. In that case, the condition for surpassing the anisotropy energetic barrier is given by $Hc \geqslant 0.5H_K$. For NPs with randomly oriented easy axes, the hysteresis cycle becomes more rounded, with remanence $M_r = 0.5M_s$, and coercivity $H_c = 0.48H_k$ [4], as shown in Fig. 1.

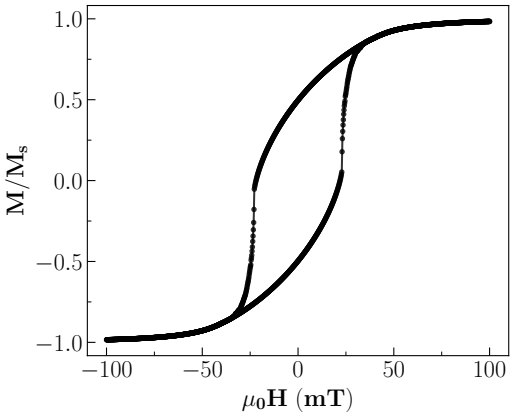

FIG. 1: Example of major hysteresis loop for an ensemble of NPs with diameter 25 and random easy axes obtained with OOMMF in agreement with the results of the SW model.

For small NPs at finite temperatures, thermal fluctuations facilitate Néel relaxation, enabling the NP magnetic moment to overcome anisotropy energy barriers and to flip under an external AMF, dissipating heat in the process. We define the Néel relaxation time as the inverse of the frequency between to minimum energy jumps:

$$\tau_N = \tau_0 e^{\frac{E_B}{K_B T}} \tag{1}$$

where $E_B = KV$ is the anisotropy energy barrier, V the particle volume and τ_0 a characteristic switching time.

Effective particle heating is observed when the "measurement time" $\tau_m \sim 1/f$ matches τ_N, causing magnetization to lag behind the applied field and to dissipate heat to the environment.

B. Pathways to SLP optimization

SLP can be optimized by enhancing the amplitude-frequency field product, choosing a material with a large saturation magnetization (M_s) and fine-tuning the magnetic properties of the NPs such as composition, shape, structure, aggregation state, and size.

The first two routes are limited by biological constraints. M_s is intrinsic to the material proposed and fixed because only bio-compatible NPs can be used. In our study, we will consider the oxide ferrite magnetite that has $M_s = 4.8 \times 10^8$ A/m $^{-1}$ and $\rho = 5170$ kg/m^3. As for the field conditions, we will consider the physiological limits imposed by the Thiesen-Jordan criterion [1] which, being less restrictive than the usually considered Brezovich criterion, will allow us to consider larger field amplitudes and, hopefully, obtain an increased SLP output.

In the hyperthermia literature, it is common to assume spherical NPs with uniaxial anisotropy, neglecting contributions from intrinsic magnetocrystalline anisotropy. This assumption is based on the idea that shape anisotropy dominates over magnetocrystalline effects. However, the latter, which is cubic and negative in the case of magnetite ($K_c = -1.1 \times 10^4$ J/m^3), is an intrinsic property of the material and can significantly influence the values of the energy barriers. In this study, we simulate ensembles of 5000 NPs under different anisotropy assumptions to investigate the role of magnetocrystalline anisotropy in the dissipated heat.

The shape anisotropy for a prolate ellipsoid (long polar c and short equatorial a axis) can be considered as a uniaxial contribution with an effective anisotropy constant K_{sh} defined as:

$$\begin{aligned} K_{\mathrm{sh}} &= \frac{\mu_0}{2}\left(N_{\mathrm{a}} - N_{\mathrm{c}}\right) M_{\mathrm{s}}^2 \\ N_c &= \frac{1}{r^2-1}\left[\frac{r}{\sqrt{r^2-1}} \ln\left(r + \sqrt{r^2-1}\right) - 1\right] \\ N_{\mathrm{a}} &= \frac{1 - N_{\mathrm{c}}}{2}, \end{aligned} \tag{2}$$

where N_a, N_c are the demagnetizing factors.

C. Simulation Model

First, to establish the model of particle ensembles, we consider magnetite NPs with sizes within the single domain limit, thus ranging from 25 to 55 nm [2]. Moreover, the NPs are assumed to be non-interacting, with their easy axis randomly oriented. Within these premises, we consider each particle to be a single superspin with magnetic moment $m = MsV$, and an effective uniaxial anisotropy K_{eff} as described by the SW model. However, contrary to this description, our simulations will include thermal fluctuations at $T = 300K$. As discussed above, we will add shape and cubic magnetocrystalline anisotropy contributions, in contrast to the assumptions of that model. To perform the simulations, we will use the OOMMF micromagnetic software [6], identifying the magnetization of each cubic discretization cell with a NP superspin. This approach has been shown to produce the correct SW results, as illustrated in Fig. 1. The software enables us to study field-driven magnetization dynamics using the Landau-Lifshitz-Gilbert equation [7, 8]:

$$\frac{d\vec{M}}{dt} = -\frac{\gamma}{1+\alpha^2}\vec{M} \times \vec{H}_{eff} - \frac{\gamma\alpha}{M_s(1+\alpha^2)}\vec{M} \times \vec{M} \times \vec{H}_{eff} \tag{3}$$

γ is the gyromagnetic factor, and α is the damping parameter, which we have fixed to 0.1. The module UHH-Evolve in OOMMF solves the equation and also adds a

stochastic thermal field to account for temperature effects.

III. RESULTS AND DISCUSSION

A. Field dependence of the SLP

Before starting the analysis regarding SLP under physiological safety conditions, we first examine the dependence of SLP on the maximum applied field at $f = 100$ kHz for two different assumptions: NPs with only uniaxial anisotropy ($K_u = K_c$), and NP with both cubic and shape anisotropy contributions with the same value. The SLP values, calculated from the simulated hysteresis loop are shown in in Fig. 2 for $f = 100$ kHz and applied fields up to 30 mT, which approaches $H_k = 48$ mT. Results for NPs with only K_c are not shown, as they yield negligible SLP in this regime. However, as it will be latter discussed in Sec. III B, this case delivers more heat than any other approximation but at higher frequencies and larger NP sizes. Under the Thiesen–Jordan criterion,

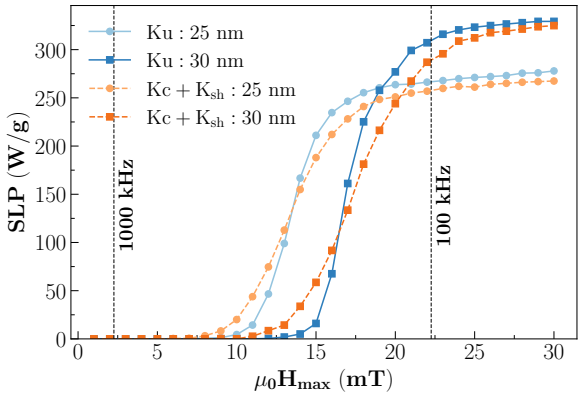

FIG. 2: SLP dependence on the maximum applied field H_{max} at a frequency $f = 100$ kHz for for NPs with diameters 25 nm (dots) and 30 nm (squares). Blue lines correspond to NPs with only uniaxial approximation $K_u = 1.1 \times 10^4$ J/m^3, dashed orange lines to NPs with cubic anisotropy $K_c = -1.1 \times 10^4$ J/m^3 and a shape contribution anisotropy with the same value. Dashed vertical lines indicate the field values for which Thiesen-Jordan is achieved at the corresponding labeled frequencies.

the field amplitude reaches its maximum at the lowest frequency. Therefore, to comply with bio compatibility limits at $f = 100$ kHz, the maximum allowable field amplitude is $\mu_0 H = 22.26$ mT. When comparing the two cases, it becomes evident that the SLP values for both K_u and $K_c + K_{sh}$ cases are quite similar, particularly for field amplitudes that maximize the field-frequency product at 100 kHz. Moreover, in contrast to prior studies based on the Brezovich criterion-where the physiologically allowed field region yielded negligible SLP [3, 9]-the present results show that the required $H_{\max}$ for significant SLP now lies within the safety threshold. This is a consequence of the less restrictive conditions imposed by the Thiesen–Jordan criterion, which allows an expanded range of field to be applied. As shown in Fig. 2, under Thiesen-Jordan conditions, the bio-compatible region (bounded by labeled vertical dashed lines) yields significant heating output. At 100 kHz, an SLP value of approximately 300 W/g is attained.

The first remarkable result in Fig.2 is that the SLP values are several times higher than those obtained under the Brezovich criterion [3]. To validate this observation, it is necessary to examine SLP behavior strictly within the Thiesen–Jordan limits. Notably, the 30 nm NP ensemble yields higher SLP than the 25 nm one, indicating that larger NP sizes may enhance heating efficiency, as energy barriers scale with volume ($E_B \propto KV$).

The influence of energy barriers also explains why the $K_c + K_{sh}$ scenario produces more SLP at low fields. The cubic anisotropy of magnetite provides 4 easy axes along the [111] directions, facilitating magnetization reversal under small fields more readily than the uniaxial case. At high fields, this same mechanism results in reduced SLP: the magnetization quickly aligns with the field, decreasing the hysteresis loop area. Conversely, in the case with only K_u, the presence of a single easy axis direction results in a higher energy barrier. Therefore, at sufficient strong fields, where the applied field can overcome the anisotropy barrier, NP ensembles with K_u will have larger hysteresis loops and thus dissipate more heat.

Understanding how changes in energy barriers affect magnetization reversal is crucial. As commented before, in the uniaxial model, energy barriers scale with both the particle volume and the anisotropy constant ($E_B \propto KV$).

Optimizing SLP thus requires a careful balance: increasing either K or V can enhance heating efficiency, but if the energy barrier becomes too large, the NP may become magnetically blocked, requiring too strong fields to achieve significant heating.

B. Size and shape influence on the SLP

This subsection further analyzes how NP size and deviations from the commonly assumed spherical shape (accounted for via a shape anisotropy contribution K_{sh}) can affect the SLP performance. Building on the NP ensemble configurations described in Sec. III A, we now analyze the impact of varying the aspect ratio r of the NP, also considering the cubic anisotropy contribution. We have considered three systems with $r = 1.09, 1.19, 1.31$ corresponding to effective shape anisotropies $K_{sh} = 5, 10, 15 \times 10^4$ J/m^3.The results are compared to cases where only cubic or only uniaxial anisotropy is included. The SLP values calculated from simulations for all five cases are shown in Fig. 3.

Compared to the results reported in [3], where the maximum SLP values were around 80 W/g, the heating power under the Thiesen-Jordan criterion reaches several hundreds of W/g (see Fig. 3), an increase of the order of 5 to 6 times with respect to the Brezovich criterion. For example, for the case of only K_u and $f = 100$ kHz,

an SLP = 50 W/g was achieved in [3], whereas in our study, the same conditions yield an SLP of 300 W/g. Moreover, for elongated NPs, a maximum SLP of 300 W/g is reached for all the studied values of r at some frequency, while under the Brezovich criterion, the maximum achievable SLP depended on r [3]. Another key

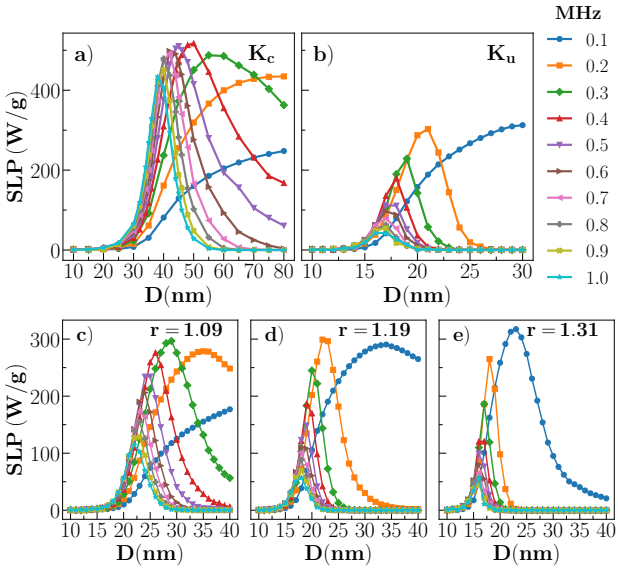

FIG. 3: Dependence of the SLP on NP diameter D and for maximum AC fields achieving the Thiesen criterion. Upper panel: NPs with only cubic (K_c, left) or only shape anisotropy (K_{sh}, right). Lower panel: ellipsoidal NPs with aspect ratios $r = 1.09, 1.19, 1.31$ as indicated.

difference from Brezovich-based results is that, while the SLP in that case was maximized at the lowest frequency (100 kHz), independently of r, in the present study this condition depends on NP elongation. This trend can be seen more clearly in Fig. 4, where the maximum SLP and the corresponding optimal diameter are plotted as functions of f. In the lower panels, the peak frequencies decrease from 300 to 200 and then 100 kHz as r increases from 1.09 to 1.31. This indicates that, under the Thiesen–Jordan criterion, , even for field amplitudes large enough that SLP peaks occur at higher frequencies, the maximum attainable SLP still depends on r. For this reason, In the $r = 1.31$ scenario, the aspect ratio may be sufficiently large so that the corresponding energy barrier can only be overcome at the maximum field amplitude (100 kHz).

As shown in Fig. 4, for elongated NPs, the maximum SLP values typically occur for NP sizes in the range $20-40$ nm over the studied frequency range. These optimal sizes are larger than those found under the Brezovich criterion, which were in the $15-28$ nm range [3]. Among the models, NPs with only K_c yield the highest SLP at all frequencies. However, note that for lower frequencies, the maximum SLP values occur for NP sizes in the range $50-80$ nm and above, approaching the single-domain limit for magnetite [2] and falling outside the range of validity of the macrospin approximation. This inverse dependence of D_{max} on f in K_c-based models can be attributed to the lower energy barrier associated with cubic anisotropy ($E \propto KV/12$) compared to the uniaxial case. Adding shape anisotropy K_{sh} on top of the cubic one shifts the maximum SLP toward smaller NP sizes. As K_{sh} increases, $\mathrm{SLP_{max}}$ decreases, and consequently $D_{\max}$ shifts to lower values, demonstrating that shape anisotropy dominates over K_c. This behavior can be explained by considering the condition for energy loss ($\tau_m \sim \tau_N$). In the uniaxial approximation, the equation for the critical volume [10] that satisfies the relaxation condition is given by:

$$V = ln\left(\frac{f_0}{f_m}\right)\frac{K_B T}{K_u}\left(1-\frac{H}{H_k}\right)^{-3/2}, \qquad (4)$$

Where an increase in K_{sh} raises the energy barrier, requiring a reduction in volume to maintain said condition.

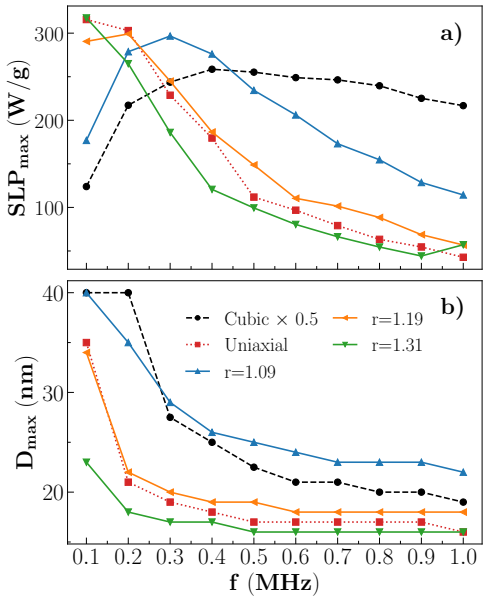

FIG. 4: Frequency dependence of SLP maximum values (a) and corresponding NP diameter at which it is attained (b), as extracted from Fig. 3.

C. Aspect ratio variability influence on the SLP

The lower panels of Fig. 3 show how different NP elongations have an impact on SLP. To examine this in more detail, we have considered simulations with aspect ratios ranging from 1.00001 (almost spherical) to 1.31 (considerably elongated), all following the Thiesen-Jordan criterion.

The results in Fig. 5 (a), (b) illustrate an initial increase in SLP with aspect ratio, displaying a peak that depends on the $H \cdot f$ product, followed by a decrease in

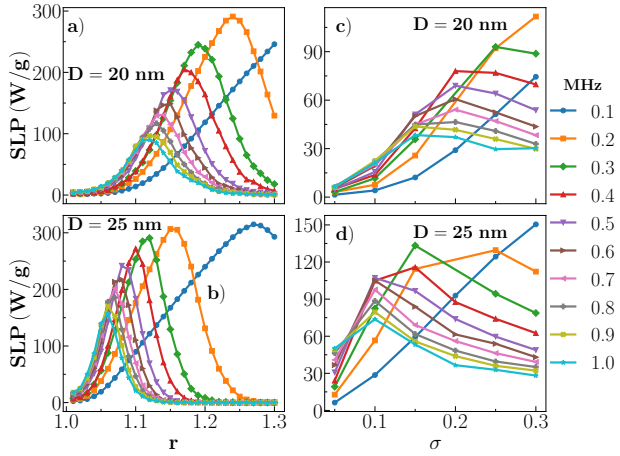

FIG. 5: Dependence of the SLP on the aspect ratio for 20 and 25 nm NPs and for maximum AC fields achieving the Thiesen-Jordan criterion shown in panels (a) and (b). Influence on SLP_{max} of ensembles with aspect ratio variability (c), (d).

SLP for larger r. The SLP increases first due to an increase in K_{sh} but, as the anisotropy constant increases, the energy barriers become higher, which leads to a mismatch of the relaxation time and AC field frequency, explaining the drop in SLP.

At larger sizes ($D = 25$ nm), there is a shift of the SLP maxima toward lower r values, indicating that the aspect ratio for which the heating is maximum decreases as the NP size increases. This is consistent with the results in III B for K_c+ K_{sh} scenarios.

In practice, it is impossible to guarantee that synthesized NP ensembles contain NP with identical aspect ratios. Therefore, we will conclude our study considering NP ensembles with aspect ratios uniformly distributed between $r = 1$ and a maximum value $r_{max} = 1+\sigma$ to see how the SLP values in this case compare with the case of a fixed r. The results are shown in panels c) and d) of Fig. 5 for two NP sizes and several frequencies.

The results in panels (a) and (b) show an increase of SLP for small σ, followed by a progressive decrease. In ensembles with high aspect ratio variability, NPs with large r present energy barriers too high to overcome, while those with small r will contribute minimally to heating, resulting in reduced overall efficiency. The optimal σ values in panels (c) and (d) correlate directly with the corresponding r_{max} in (a) and (b). For $D = 25$ nm, the optimal aspect ratio is approximately $r_{\max} \sim 1.1$, with an optimal variability range of $\sigma \sim 0.1$–0.15. In contrast, for $D = 20$ nm, $r_{\max} \sim 1.15$–1.20, with an optimal σ range of approximately 0.15–0.20. This suggests that efficient heating requires narrow r distributions centered around the optimal r value. For $D = 20$ nm, the σ peaks are less pronounced than those for $D = 25$ nm. This difference arises because the simulations increase r starting from $r = 1.00001$. This method works well for $D = 25$ nm, where the optimal $r_{\max} \sim 1.1$ is close to the starting point. However, for $D = 20$ nm, where r_{max} is significantly higher, starting the distribution near $r = 1.0$ makes the optimization unclear.

IV. CONCLUSIONS

Our findings highlight the importance of considering the $H \cdot f$ product criterion in simulation studies of realistic magnetic hyperthermia models. Compared to Brezovich criterion, SLP values obtained using the Thiesen-Jordan criterion increase by a factor of 5 to 6, significantly enhancing heating efficiency. A primary objective of this study was to assess the suitability of the commonly used uniaxial-only anisotropy model for describing hyperthermia performance under Thiesen-Jordan conditions. Our results show that magnetocrystalline anisotropy plays a significant role in determining the SLP efficiency and that it must be explicitly considered. Moreover, our simulations including shape anisotropy(K_{sh}) demonstrate that even slight deviations from spherical geometry can significantly influence SLP performance. The results for the dependence of SLP on both NP size and aspect ratio variability in NP ensembles underscore the importance of precisely controlling these parameters in NP design strategies for hyperthermia treatment. In particular, reduced aspect ratio variability within NP ensembles is shown to promote more uniform heating across the NP ensembles, yet leading to optimal therapeutic heating output.

Acknowledgments

I would like to express my sincere gratitude to my advisor, Dr. Òscar Iglesias for his patience and guidance in this work. I also acknowledge CESGA and CSUC for the computational resources that made this study possible.

[1] B. Thiesen and A. Jordan, Inter. J. Hyperth. **24**, 467 (2008).
[2] R. Hergt *et al.*, J. Phys. Condens. Matter **18**, S2919 (2006).
[3] D. Faílde *et al.*, Nanoscale **16**, 14319 (2024).
[4] E. Stoner and E. Wohlfarth, Philos. Trans. R. Soc. A **240**, 599 (1948).
[5] K. M. Krishnan, *Fundamentals and Applications of Magnetic Materials* (Oxford University Press, 2016).
[6] M. J. Donahue and D. G. Porter, NIST, Gaithersburg, MD **1**, 157 (1999).
[7] L. Landau and E. Lifshitz, Phys. Z. Sowjetunion **8**, 153 (1935).
[8] T. Gilbert, IEEE Transactions on Magnetics **40**, 3443 (2004).
[9] H. Gavilán *et al.*, Nanoscale **13**, 15631 (2021).
[10] R. H. Victora, Phys. Rev. Lett. **63**, 457 (1989).

Optimització de la hipertermia magnètica sota condicions segures de camp

Carlota Puig Acevedo, cpuigace7@alumnes.ub.edu
Facultat de Física, Universitat de Barcelona, Diagonal 645, 08028 Barcelona, Spain.

Advisor: Òscar Iglesias, oscariglesias@ub.edu

Resum: Una avaluació precisa de l'escalfament de les nanopartícules magnètiques (NPM) sota camps AC és essencial per optimitzar els tractaments de hipertèrmia dins dels límits fisiològicament segurs. L'estudi d'aquest treball es basa en la simulació de sistemes de NPM amb variacions de mida i anisotropia per tal d'analitzar-ne el comportament sota diferents condicions de camp extern. Per estudiar l'evolució temporal del camp magnètic i la dinàmica de la magnetització del sistema, s'ha utilitzat el model micromagnètic basat en l'equació de Landau-Lifshitz-Gilbert, implementat al programari OOMMF. Els models usuals es fonamenten en l'ús de l'aproximació d'anisotropia uniaxial, on l'escalfament de les NPM està dominat pels efectes de forma. Tanmateix, les nostres simulacions mostren que el model convencional falla quan s'apliquen camps de baixa amplitud dins els límits fisiològics acceptats. En aquestes condicions, els resultats mostren que la anisotropia magnetocristal·lina té un impacte no negligible en la generació de potencia específica dissipada, i que desviacions petites respecte a la forma esfèrica influencien significativament l'eficiència de l'escalfament. Els resultats, avaluats sota el criteri de Thiesen-Jordan, confirmen que un funcionament òptim de la hipertèrmia requereix models que incorporin tan l'anisotropia de forma com la intrínseca, així com una distribució de mida adient i una mínima variabilitat de forma de les NP.
Paraules clau: Nanopartícules magnètiques, micromagnetisme, histèresi, tractament de càncer, aplicacions biomèdiques, mètodes de simulació
ODSs: Salut i benestar, educació de qualitat i indústria, innovació, infraestructures.

Objectius de Desenvolupament Sostenible (ODSs o SDGs)

1. Fi de la es desigualtats		10. Reducció de les desigualtats	
2. Fam zero		11. Ciutats i comunitats sostenibles	
3. Salut i benestar	X	12. Consum i producció responsables	
4. Educació de qualitat	X	13. Acció climàtica	
5. Igualtat de gènere		14. Vida submarina	
6. Aigua neta i sanejament		15. Vida terrestre	
7. Energia neta i sostenible		16. Pau, justícia i institucions sòlides	
8. Treball digne i creixement econòmic		17. Aliança pels objectius	
9. Indústria, innovació, infraestructures	X		

El contingut d'aquest TFG, part d'un grau universitari de Física, es relaciona amb l'ODS 3, i en particular amb la fita 3.4 ja que contribueix a la reducció de la mortalitat prematura per malalties no transmissibles, en aquest cas el càncer, mitjançant el tractament (hipertèrmia). També es pot relacionar amb l'ODS 4, fita 4.4 vist que contribueix a l'educació a nivell universitari. Finalment amb l'ODS 9, fita 9.5, perquè promou la transferència de coneixement científic cap a aplicacions pràctiques i el desenvolupament de tècniques terapèutiques.